Proceedings of the ASME 2010 3rd Joint US-European Fluids Engineering Summer Meeting and 8th International Conference on Nanochannels, Microchannels, and Minichannels
FEDSM-ICNMM2010
August 1-5, 2010, Montreal, Canada

FEDSM-ICNMM2010-30070

A FINITE ELEMENT MODEL FOR PREDICTING THE COLLAPSE OF SHORT AND LARGE TWO-LINE PATTERNS DURING DRYING PROCESS IN PHOTOLITHOGRAPHY

Seyed Farshid Chini
Department of Mechanical Engineering,
University of Alberta
Edmonton, AB, Canada

Alidad Amirfazli
Department of Mechanical Engineering,
University of Alberta
Edmonton, AB, Canada

ABSTRACT
Photolithography is one of the main mass nano-production processes. Smaller devices are always aimed to save material and energy. Manufacturing small devices by photolithography is a challenge, due to the risk of collapse of patterns during the drying of rinse liquid. One of the main pattern shapes is the two-line parallel. In our previous study, an analytical model was developed for predicting the collapse of large (L/d, *LAR*>20; see Fig. 1) two-line parallel patterns [1]. This model assumes the rinse interface shape is cylindrical. Knowledge of the rinse interface shape is needed to define the forces contribute to collapse, *i.e.* Laplace pressure and surface tension force at the three-phase line.

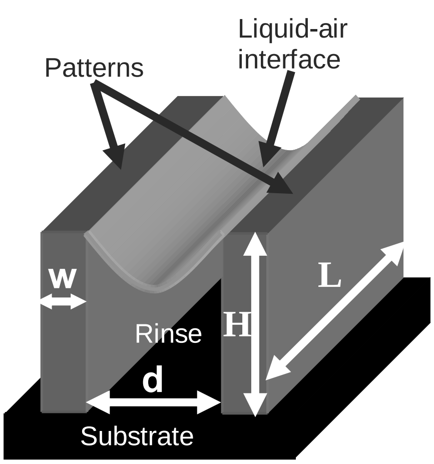

Figure 1 A two-line parallel pattern is shown.

In the current study, a Finite Element (FE) model is developed to predict the collapse of short (*LAR*<20) and large (*LAR*>20) two-line parallel patterns. Rinse liquid shape and its curvature are found using Surface Evolver (an interactive program for the study of surfaces shaped by surface tension, gravitational and other energies). Another finite element method (*i.e.* ANSYS 11.0) is used to find the pattern deformation. It was found that the pattern deformation decreases by decreasing the *LAR* value. It is important as for the cases that due to the design specifications, selection of the pattern material and rinse liquid is restricted, by changing the *LAR* value one may resolve the collapse problem.

KEYWORDS
Pattern collapse, Photolithography, MEMS Sticktion, L-shaped patterns, Capillary forces.

INTRODUCTION
One of the most efficient methods for manufacturing the micro- and nano-scale features is photolithography. In the photolithography process, silicon oxide is covered by the photoresist material, and then exposed to the UV (ultra violet) light through a photomask. Depending on the photoresist type, exposed or unexposed parts of the photoresist dissolve in the developer which is mainly water. During the acid etching, the remained photoresist acts as a sacrificial layer and keeps the underneath silicon oxide layer intact. So, the pattern on the photomask is replicated into the silicon oxide wafer. One of the main obstacles in photolithography process for producing fine features is collapse of photoresist patterns during drying of the developer (or rinse) liquid [2]. The collapse reason is reported as unbalanced capillary forces during non-uniform drying of the rinse liquid [3,4 and 5]. The contributors to capillary forces are Laplace pressure and surface tension force (STF) [1].

SURFACE TENSION FORCE
Surface tension force is a concentrated force on the three-phase line. Three-phase line is the confluence zone of the liquid, solid and gas phases described by a line. The value of the SFT is equal to the value of the rinse liquid-air surface tension (γ_{LV}). STF or γ_{LV} is in the direction tangent to the air-liquid interface (Fig. 2a). Extrand *et al.* [6] showed that the magnitude of the

STF is such that it can deform a polymeric substrate at the three-phase line and form a ridge; in case of a sessile drop placed on a soft surface (Fig. 2b). For the purpose of the pattern collapse study, the projection of the STF normal to the pattern's side wall is of interest (see Fig. 2a). The reason is that the projection of the STF parallel to the pattern's side wall is cancelled by other interfacial surface tensions according to the Young's equation (see Eq. 1).

$$\gamma_{LV}\cos\theta + \gamma_{SL} = \gamma_{SV} \tag{1}$$

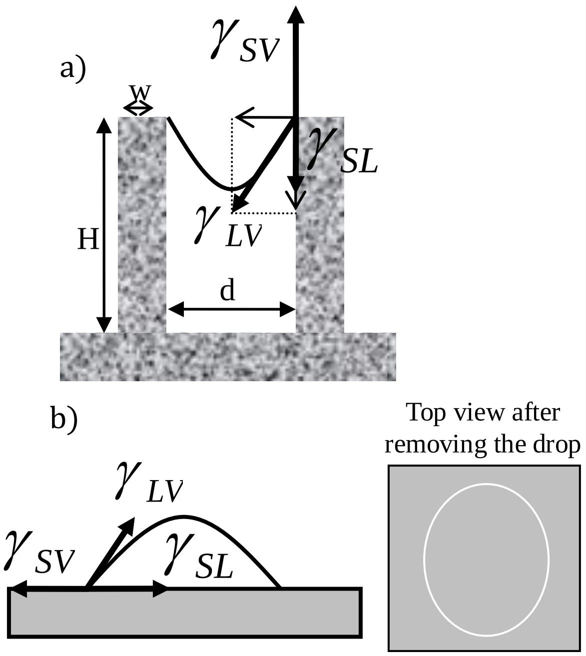

Figure 2(a) Horizontal projection of γ_{LV} is exerting a force on the pattern while its vertical projection, according to Young equation, is canceled by two other interfacial tensions, *i.e.* γ_{SL} and γ_{SV} . (b) Extrand *et al.* [6] experiment, *i.e.* a drop on a soft substrate. White circle signifies a ridge that was formed at the three-phase line on a soft substrate. It shows that the magnitude of the STF is such that it can deform a soft substrate.

LAPLACE PRESSURE

Laplace pressure (ΔP) is the pressure difference across the interface of the rinse liquid and air. Laplace pressure is a function of the interface curvature (κ) and surface tension of the rinse liquid (γ), as described by Eq. 2 [7,8 and 9].

$$\Delta P = \gamma.\kappa \tag{2}$$

For the cases that liquid is trapped inside the patterns, and interface of the rinse liquid is concave (*e.g.* Fig.2a), Laplace pressure is negative which means that the pressure inside the rinse liquid is lower than the outside pressure. So, Laplace pressure pulls the patterns towards each other [10, 11 and 12]. Assuming cylindrical shape for the rinse interface and using goniometry, Laplace pressure would be [13, 14, 15 and 16]:

$$\Delta P = \frac{2\gamma\cos(\theta-\phi)}{d-2\delta} \tag{3}$$

where ϕ is the slope angle of the pattern at its three-phase line, θ is the contact angle (angle between the rinse liquid interface and pattern's side wall) and δ is the pattern deformation at the three-phase line. Besides the Laplace pressure value, to identify the pattern deformation, the area exposed to the Laplace pressure is essential. The area is defined and delimited by the three-phase line.

Chini *2008* [1] showed that for two-line parallel patterns with *LAR* values larger than 20, assuming a cylindrical interface shape for the interface is valid. Then, by modeling the patterns as beams and applying the beam bending relations, deformation can be found by solving the following closed form equation (Eqs. 4 and 5).Total deformation of the pattern would be the summation δ_1 and δ_2.

$$\frac{\dfrac{\cos\theta\left(1-\dfrac{12\delta_1\delta_2}{6H^2}\right)+\sin\theta\left(\dfrac{3\delta_2}{2H}+\dfrac{4\delta_1}{3H}\right)}{d-2(\delta_1+\delta_2)}}{\sqrt{\left(\left(\dfrac{3\delta_2}{2H}\right)^2+1\right)\left(\left(\dfrac{4\delta_1}{3H}\right)^2+1\right)}} = \frac{Ew^3}{3\gamma H^4}\delta_1 \tag{4}$$

$$\delta_2 = \frac{4\gamma H^3\sin\theta}{Ew^3} \tag{5}$$

For *LAR* values smaller than 20, assuming a cylindrical interface shape for the interface is inaccurate in predicting the precise interface curvature value and three-phase line shape. Also, modeling the pattern as a beam is only valid where pattern has a line shape *e.g.* two-line parallel patterns. As such, using the analytical model of [1] is invalid to predict the deformation of following pattern geometries: short two-line parallel and L-shaped patterns (these geometries are shown in [17]). For these cases, a Finite Element (FE) model will be developed to calculate the pattern deformation.

MODELING ASSUMPTIONS

The pattern dimensions studied in this study are in consideration of international technology roadmap for semiconductors or Moore's law which states that the number of transistors on a chip doubles every 18 months [18]. In 2007 desirable ½ pitch of patterns was 65nm (trough width (*d*) and pattern width (*w*) in Fig.1 were 65nm) and should shrink to 40nm by the end of 2011 [19].

In this study bulk values are used for studying the photoresist material however for example Goldfarb *et al.* [20] stated that elasticity modulus of nano-photoresist deviates from its bulk value. Nevertheless, for improvement, nano-scale values may be substituted with bulk values in the future.

Pattern deformation is assumed linearly elastic and touching of the tips of two adjacent patterns or the start of plastic deformation are the collapse criteria (whichever occurs first). However, in some cases before pattern tips touch or plastic deformation starts, patterns, at the pattern base, might detach from the substrate and cause collapse. This happens due to the improper pre-baking process. The current model is not able to predict this type of collapse. For improving the model, to consider the pattern's base detachment from the substrate scenario, maximum tolerable stress of the base should be defined and compared with the stress exerted at the base.

For some applications small plastic deformation of the pattern is permitted. As such, the pattern with that small plastic deformation may not be considered as collapsed. However, the FE models predict collapse for such a case. The current FE model may be upgraded to account for some specific plastic deformations.

The effect of evaporation of the rinse liquid through changing the rinse liquid volume and contact angle is disregarded in current model. Volume decrease due to the evaporation of rinse liquid, changes the contact angle [21] used in beam bending or FE models. In other words, as the level of the rinse liquid inside the pattern goes down, receding contact angle, which is smaller than the equilibrium contact angle, should be used in the model. Contact angle defines the Laplace pressure and horizontal projection of STF.

Due to the rinse liquid penetration into the pattern, contact angle value and pattern stiffness may change (depending on the diffusion amount). Contact angle or stiffness changes due to swelling are disregarded in current simulation model. Forthcoming models may simulate the diffusion into the pattern to find the pattern stiffness as a function of time.

To consider the worst case scenario, the rinse volume at which the maximum possible pattern deformation happens is considered in the FE model. From SE, it is observed that the Laplace pressure value, the area exposed to the pressure, and contact line location change with changing the rinse liquid volume (Fig. 3). Increasing the Laplace pressure value, pattern area exposed to the pressure and contact line rise, results in pattern deformation increase. It was found that the maximum possible capillary force happens where the pattern's side wall is completely wet; and Laplace pressure is uninfluenced by the overfilling effect *i.e.* panel b in Fig. 3 (this observation is tested for *d*=*w*=32, 45, 57, 65 and 104 nm for both two-line parallel and L-shaped patterns). It should be noted that the analytical model of [1] was independent of the rinse liquid volume, as it was a simplified approach and interface shape was assumed cylindrical.

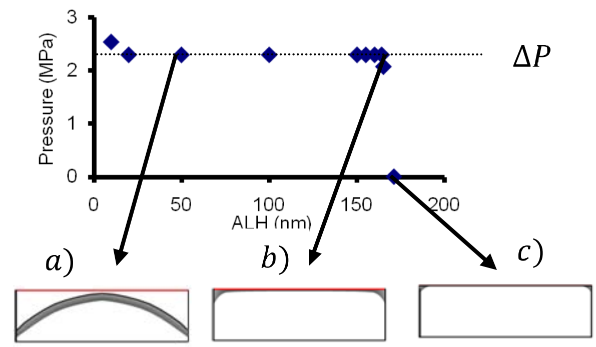

Figure 3 Laplace pressure, three-phase line (thick black lines in three panels) and interface shapes (gray shades) of a two-line parallel pattern at different *ALH* (average liquid height) values are shown. For the case "b", three-phase line is a straight line and pressure value is not influenced by the overfilling effect. *AR* (=*H/w*, shown in Fig. 1) =3, *LAR*=10, *d*=*w*=57nm (state of the art for 2008), $\theta = 5^o$, $\gamma = 72.9mN/m$.

CREATING THE MODEL AND CALCULATING THE DEFORMATION

The procedure of finding the deformation in Finite Element model is as follow (see Fig. 4): (i) the geometric model is created in Surface Evolver (SE, a software capable of generating accurate interface shapes by knowing interface energies [22,23]) to find the rinse liquid interface shape and subsequently Laplace pressure value (using Eq. 2); (ii) applying the capillary forces (*i.e.* Laplace pressure and STF) to the geometric model created in ANSYS 11.0 (a widely known FE package capable of finding stress, strain and deformation distributions[24]); (iii) finding the deformed shape of the pattern; (iv) resume from step i, updating the interface shape based on the pattern deformation. This procedure continues till the deformation converges within a range of 1%.

The deformation value from FE may or may not converge. If the deformation from FE model converged to a value smaller than half of the trough width, pattern is not considered collapsed. Non-convergence or convergence to a value larger than half of the trough width signifies the pattern collapse.

Slope angle and deformation of the pattern at the tip are the data needed to import the deformed pattern shape into the Surface Evolver. As such an element capable of providing both the slope angle and deformation is selected in ANSYS (*i.e.* Shell43). For the cases selected to study (*i.e.* state of the art dimensions for 2007 to 2011) it was observed that slope of the pattern at the tip even at the moment of collapse, or maximum possible deformation, is negligible (less than 4 degrees, *e.g.* see Fig. 6a). As the value of slope angle is small, to simplify the complicated simulations, slope angle can be ignored. Therefore, one may choose easier to apply elements in ANSYS (*e.g.* Solid95) and obtain accurate enough pattern deformation values. After development of the FE model, the model needs to be tested with the cases that the pattern deformation values were known.

VALIDATION OF THE FE MODEL RESULTS

To verify the FE model (developed in section 2) and see whether for example correct solver method, element and meshing are used, FE and analytical model of [1] results are compared, for two-line parallel patterns with *LAR* value larger than 20 (the analytical model was suggested for two-line parallel patterns with *LAR>20*). It should be noted that for the cases that pattern deformation is very large, analytical model of [1] is inaccurate. The reason is that the analytical model of [1] is based on the small deformation assumption (capillary forces remain horizontal instead of rotating and remaining perpendicular to the pattern's side wall during the deformation).

As expected, the FE and analytical model results are close (within 5%, see Fig. 5), but not equal. The difference between analytical model of [1] and FE increases by changing any factor which leads to increasing the deformation (*e.g.* see Fig. 5). Regarding Fig. 5 it should be noted that analytical model of [1] is different from Tanaka *et al.* 1993 beam bending model as Tanaka's beam bending model neglects the STF effect on the pattern deformation.

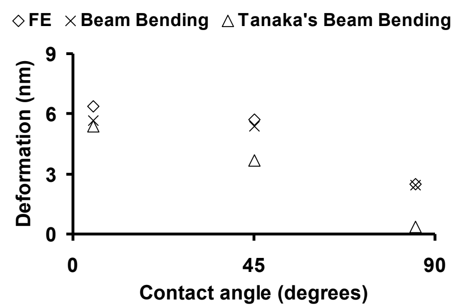

a)

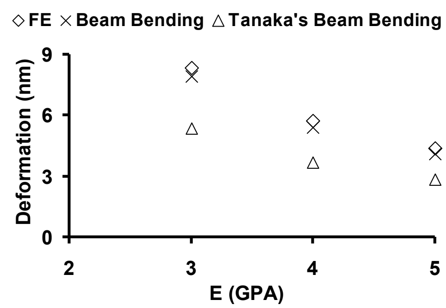

b)

Figure 4 Deformations of a two-line parallel pattern from beam bending or [1] , Tanaka's beam bending and FE model are compared at (a) different contact angles with Elasticity modulus, *E*=4GPa, (b) different *E* values with $\theta = 45^o$. *d*=*w*=57nm, *AR*=3, $\gamma = 72.9mN/m$ and $LAR \to \infty$.

The FE model is able to find the deformation of two-line parallel with short (*LAR<20*) length patterns where analytical models is ineffective.

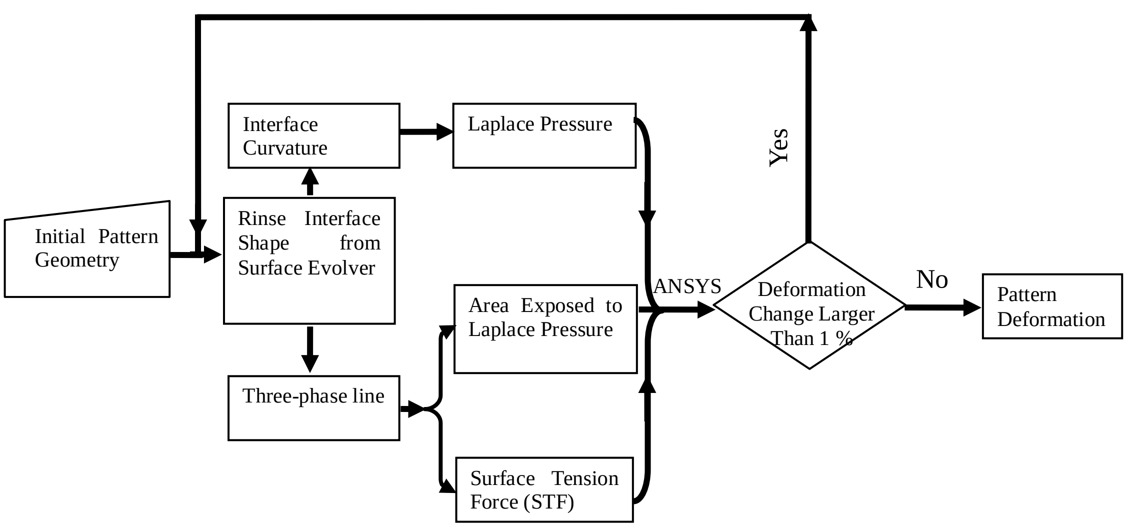

Figure 5 Procedure of calculating pattern deformation using FE method is shown.

SHORT TWO-LINE PARALLL PATTERNS

For the case of two-line parallel patterns, it was found that by decreasing the *LAR* value, pattern deformation decreases (regardless of the contact angle; *e.g.* see Fig. 6b). By decreasing the *LAR* value, Laplace pressure value decreases. It should be noted that the effect of *LAR* on changing the Laplace pressure was neglected in analytical model of [1]. So, for the cases that design and application limit the change of rinse liquid or photoresist material, change of *LAR* may be an alternative to resolve the collapse problem for two-line parallel patterns, if functional design of the device being fabricated allows.

a)

b)

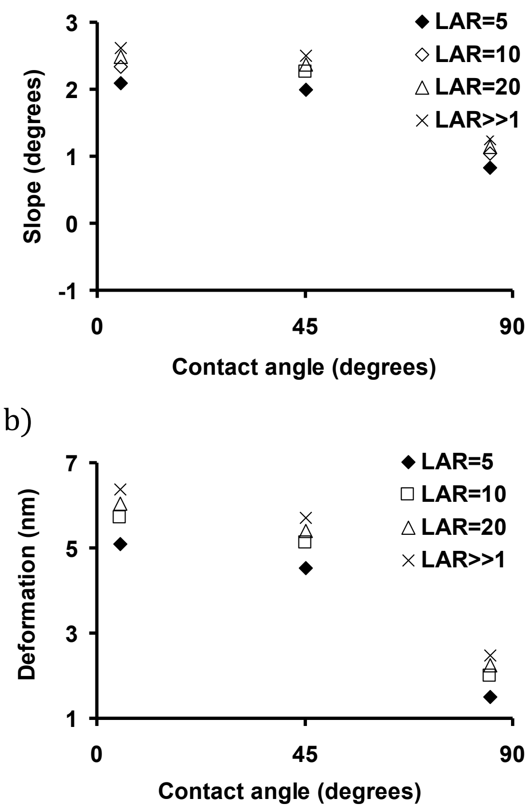

Figure 6 (a) Slope of the pattern at its tip and (b) deformation at different contact angles is shown for different *LAR* values (d=w=57nm, *AR*=3, $\gamma = 72.9mN/m$, *E*=4GPa and two-line parallel pattern).

It was found that for any contact angle value, there exists an *LAR* value at which interface becomes flat or Laplace pressure becomes zero. In this study the *LAR* value at which rinse interface curvature becomes zero is named the "transition *LAR"* value. It is found that for small contact angles the "transition *LAR"* value decreases. For example, "transition *LAR"* value is approximately 10 for contact angle of 85 degrees and 1 for contact angle of 5 degrees.

At the "transition *LAR"*, Lapace pressure is zero but STF is still operative on the pattern's side wall. For *LAR* values lower than the transition *LAR*, curvature value is positive and Laplace pressure drives out the two adjacent patterns from each other (pressure inside the rinse liquid is higher than the outside pressure). Therefore, effects of Laplace pressure and STF are opposite to each other which may be used to have very small pattern deformations (*e.g.* for the specific case of two-line parallel pattern with *w=d=65nm* ,state of the art for 2007, *LAR*=5, and $\theta = 85^o$, deformation is approximately 1nm). The ideal case would be where the deformation due to the Laplace pressure and STF cancel out each other.

CONCLUSION

Analytical models developed in the literature (*e.g.* [1]) model the pattern as a beam, rinse interface shape is modeled as a part of a cylinder; and small deformation assumption is used. Therefore, the models are limited to a specific case of two-line parallel pattern with *LAR* values larger than 20 with small deformation. The error of the analytical model for two-line parallel patterns with *LAR>20* may not be negligible for large deformations.

In this study, a pattern geometry, where analytical models were unable to predict the pattern deformation, is defined (*i.e.* two-line parallel with short length, *LAR*<20). For this pattern geometry, the rinse interface cannot be modeled as a part of a cylinder. A coupled Finite element model using Surface Evolver and ANSYS is developed to calculate the pattern deformation value for these cases. The FE model was validated using analytical model of [1] (for two-line parallel patterns with *LAR*>20). It was found that the pattern deformation decreases by decreasing the *LAR* value. It is important as for the cases that due to the design specifications, selection of photoresist material and rinse liquid is restricted, by changing the *LAR* value one may resolve the collapse problem.

ACKNOWLEDGMENTS

Authors of this paper would like to thank NSERC and Canada research chair program for their financial support.

REFERENCES

1. S. F. Chini, *Pattern Collapse in Photolithography Process*, MSc Thesis, University of Alberta, 2008.
2. K. Deguchi, K. Miyoshi, T. Ishi and T. Matsuda, Jpn. J. Appl. Phys., 31, 2954-8, (1992)
3. T. Tanaka, M. Morigami and N. Atoda, Jpn. J. Appl. Phys., 32, 6059-6064, (1993)
4. M. Kotera, N. Ochiai, J. Microelect. Eng., 78-79, 515-520, (2005)

5. K. Yoshimoto, M. P. Stoykovich, H. B. Cao, J. J. de Pablo, P. F. Nealey and W. J. Drugan, J. Appl. Phys., 64, 1857-1865, (2004)
6. C. W. Extrand and Y. Kumagai, J. Colloid Interafce Sci., 184, 191-200, (1996)
7. H. B. Cao and P. F. Nealey, J. Vac. Sci. Technol. B, 18, 3303-3307, (2000)
8. Ki-Soo and G. Lee, J. Photopolymer Sci. Tech., 16, 363-368, (2003)
9. M. P. Stoykovich, H. B. Cao, K. Yoshimoto, L. E. Ocola and P. F. Nealey, Adv. Mater. 15, 1180-1184, (2003)
10. Y. Jincao, M. A. Matthews and C. H. Darvin, Ind. Eng. Chem. Res., 40, 5858-5860, (2001)
11. K. D. Vora, B. Y. Shew, E. C. Harvey, J. P. Hayes and A. G. Peele, J. Micromech. Microeng., 15, 978-983, (2005)
12. A. Drechsler, C. Bellmann, A. Synytska, N. Petong, K. Grundke, M. Stamm, J. Reichelt and O. Wunnicke, J. Colloids and Surfaces A Physiochem. Eng., 311, 83-92, (2007)
13. I. Junarsa, M. P. Stoykovich, K. Yoshimoto and P. F. Nealey, Proc. SPIE Conf. on Advances in Resist Technology and Processing XXI, Bellingham, WA, USA, (2004)
14. Hyung-Joo Lee, Jun-teak Park, Ji-yong Yoo, Ilsin An and Hye-Keun Oh, Jpn. J. Appl. Phys., 42, 3922-3927, (2003)
15. S-K Kim, J. Korean Phys. Soc., 42, S371-S375, (2003)
16. D. L. Olynick, B. D. Harteneck, E. Veklerov, M. Tendulkar, J. A. Liddle, A. L. D. Kilcoyne and T. Tyliszczak, J. Vac. Sci. Technol. B, 22, 3186-3190, (2004)
17. T. Ito, K. Kadota, M. Nagao, A. Sugimoto, M. Nozaki and T. Kato, J. Vac. Sci. Technol. B, 8, 1080-1086, (1990)
18. www.itrs.net/Links/2006Update/FinalToPost/08_Lithography2006Update.pdf, last accessed on 15 December 2009
19. www.itrs.net/Links/2006Update/FinalToPost/08_Lithography2006Update.pdf, last accessed on 15 December 2009
20. D. L. Goldfarb, M. Angelopoulos, E. K. Lin, R. L. Jones, C. L. Soled, J. L. Lenhart and Wen-li Wu, J. Vac. Sci. Technol B 19, 2699-2703 (2001)
21. Jung-Hoon Kim, S. I. Ahn, J. H. Kim and Wang-Cheol Zin, J. Langmuir, 23, 6163-6169 (2007)
22. D. Chatain, D. Lewis, J. P. Baland and W. C. Carter, Langmuir, 22, 4237-4243, (2006)
23. www.susqu.edu/brakke/evolver, last accessed on 15 December 2010
24. ANSYS, Inc. USA, www.Ansys.com, last accessed on 15 December 2010